Electric dipole polarizability of group-13 ions using perturbed relativistic coupled-cluster theory: Importance of nonlinear terms

Ravi Kumar,[1] S. Chattopadhyay,[2] B. K. Mani,[1] and D. Angom[3]
[1]*Department of Physics, Indian Institute of Technology, Hauz Khas, New Delhi 110016, India*
[2]*Department of Physics, Kansas State University, Manhattan, Kansas 66506, USA*
[3]*Physical Research Laboratory, Ahmedabad - 380009, Gujarat, India*

(Received 16 April 2019; revised manuscript received 6 December 2019; published 6 January 2020)

We compute the ground-state electric dipole polarizability α of the group-13 ions using the perturbed relativistic coupled-cluster theory. To account for the relativistic effects and quantum electrodynamical corrections, we use the Dirac-Coulomb-Breit Hamiltonian with the corrections from the Uehling potential and the self-energy. The effects of triple excitations are considered perturbatively in the theory. Our results for polarizability are in good agreement with previous theoretical results for all the ions. From our results we find that the nonlinear terms in perturbed relativistic coupled-cluster theory have significant contributions and must be included to obtain accurate value of dipole polarizability for group-13 ions. For the correction from the Breit interaction, we find that it is largest for Al^+ and decreases with increasing Z. The corrections from the vacuum polarization and the self-energy increases with increasing Z.

DOI: 10.1103/PhysRevA.101.012503

I. INTRODUCTION

The electric dipole polarizability of atoms or ions is a measure of the interaction with an external electromagnetic field [1]. It is a key parameter, and plays an important role in probing fundamental as well as technologically relevant properties of atoms and ions. Some current and potential implications of α in atomic systems include discrete symmetry violations in atomic systems [2,3], optical atomic clocks [4,5], condensates of dilute atomic gases [6–8], high-harmonic generation and ultrafast processes [9–12], and the search for the variation in the fundamental constants [13].

The recent advances in the development of new and improved frequency and time standards in optical domain has increased interest in the electric dipole polarizability of atoms and ions. One of the important reasons for this is that the electric dipole polarizability (α) is essential to calculate the blackbody radiation (BBR) shift in the atomic or ionic transition frequencies due to ac Stark effect. The BBR shift is one of the dominant environment induced shifts in atomic transition frequency, and contributes to the inaccuracy of atomic clocks. Here, it is to be emphasized that the group-13 ions are promising candidates for accurate optical atomic clocks as they are expected to have low fractional frequency errors [14–18]. Here, it is to be mentioned that we have used the IUPAC nomenclature to identify the group in the periodic table [19]. Among the ions in the group, an optical atomic clock with Al^+ has recently reached the fractional frequency uncertainty of 9.4×10^{-19} [20,21]. This is, perhaps, the most precise clock in existence today. Despite the important prospect associated with these ions, the ground-state polarizability has not been studied in detail. For example, except for Al^+, very little data is available from the previous theoretical calculations. This, perhaps, can be attributed to the complex nature of the correlation effects in these divalent ions.

It can thus be surmised that there is a research gap on the dipole polarizability for group-13 ions. But, considering the experimental developments there are compelling reasons to address this research gap. That is the aim of this work. For this we employ the perturbed relativistic coupled-cluster (PRCC) theory and compute the ground state α of group-13 ions and examine the trends in correlation effects in detail. More precisely, our aim is to compute accurate value of α for B^+, Al^+, Ga^+, In^+, and Tl^+ ions using PRCC theory; examine in detail the contributions from the nonlinear terms in PRCC theory; do a comparative study with the trends observed in other closed-shell atoms and ions [22–27]; and examine the contributions to α from Breit interaction, vacuum polarization and the self-energy corrections, and compare them with other closed-shell atoms and ions. Such a study is essential, as mentioned in Ref. [20], to obtain accurate values of the BBR shift to reduce the uncertainty of Al^+ optical atomic clocks. And, the same reasoning applies to the other ions of the group. In particular, the importance of obtaining accurate values of α is that the BBR shift depends on the differential polarizability [28]. Hence, obtaining reliable value of the ground-state polarizability is essential.

The PRCC theory is an appropriate many-body theory to account for the correlation effects arising from the external perturbation. It has been used to compute accurate value of α for several atoms and ions in a series of our previous works [22–27]. The essence of PRCC is that it is a relativistic coupled-cluster (RCC) theory [29–31] with an additional set of cluster operators. The latter accounts for the effects of an internal or external perturbation Hamiltonian. The amplitudes of these cluster operators are obtained by solving a new set of coupled linear equations; this is in addition to the RCC cluster amplitude equations. The added advantage of PRCC is that it does not employ the sum-over-state [32,33] approach to incorporate the effects of a perturbation. The summation

over all the possible intermediate states is subsumed in the perturbed cluster operators. In our previous works we have also demonstrated and verified the implementations of the Breit interaction [23], vacuum polarization [25], and triple excitation in unperturbed [26] and perturbed [27] cluster operators. In the literature, there are other many-body theories which have been used to compute α to good accuracy for a variety of atomic systems. A recent review by Mitroy and collaborators [34] provides a detailed overview of these many-body theories and their applications. The remaining part of the paper is organized as follows. In Sec. II we provide an overview of the RCC and PRCC theories. In Sec. III we provide the calculational details where we discuss the basis functions, nuclear potential, etc., used in the present work. The results obtained from our computations are analyzed and discussed in Sec. IV. Unless stated otherwise, all the results and equations presented in this paper are in atomic units($\hbar = m_e = e = 1/4\pi\epsilon_0 = 1$).

II. THEORETICAL METHODS

We use the Dirac-Coulomb-Breit no-virtual-pair Hamiltonian $H^{\rm DCB}$ to incorporate the relativistic effects in high-Z atoms. It provides a good description of the structure and properties of heavier atoms and ions. For an N-electron atom or ion,

$$H^{\rm DCB} = \sum_{i=1}^{N}[c\boldsymbol{\alpha}_i\cdot\mathbf{p}_i + (\beta_i - 1)c^2 - V_N(r_i)] + \sum_{i<j}\left[\frac{1}{r_{ij}} + g^{\rm B}(r_{ij})\right], \tag{1}$$

where $\boldsymbol{\alpha}$ and β are the Dirac matrices. In the present work the negative-energy continuum states of the Hamiltonian are projected out by using the kinetically balanced finite GTO basis sets [35,36], and selecting only the positive energy states from the finite size basis set [37,38]. The last two terms, $1/r_{ij}$ and $g^{\rm B}(r_{ij})$, are the Coulomb and Breit interactions, respectively. The Breit interaction, which represents the interelectron magnetic interactions, is

$$g^{\rm B}(r_{12}) = -\frac{1}{2r_{12}}\left[\boldsymbol{\alpha}_1\cdot\boldsymbol{\alpha}_2 + \frac{(\boldsymbol{\alpha_1}\cdot\mathbf{r}_{12})(\boldsymbol{\alpha_2}\cdot\mathbf{r}_{12})}{r_{12}^2}\right]. \tag{2}$$

The Hamiltonian $H^{\rm DCB}$ satisfies the eigenvalue equation,

$$H^{\rm DCB}|\Psi_i\rangle = E_i|\Psi_i\rangle, \tag{3}$$

where $|\Psi_i\rangle$ is the exact atomic state and E_i is the corresponding exact energy.

In the presence of external perturbations, the Hamiltonian $H^{\rm DCB}$ is modified with the addition of the perturbation interaction terms. For example, the total Hamiltonian in the presence of an external electric field $\mathbf{E}_{\rm ext}$ is

$$H_{\rm Tot} = H^{\rm DCB} + \lambda H_{\rm int}, \tag{4}$$

where $H_{\rm int} = -\mathbf{D}\cdot\mathbf{E}_{\rm ext}$ is the interaction Hamiltonian, arising from the interaction between the induced electric dipole moment $\mathbf{D}$ of the atom and the external electric field $\mathbf{E}_{\rm ext}$. And, λ is a perturbation parameter. The modified Hamiltonian satisfies the eigenvalue equation,

$$H_{\rm Tot}|\tilde{\Psi}_i\rangle = \tilde{E}_i|\tilde{\Psi}_i\rangle, \tag{5}$$

where $|\tilde{\Psi}_i\rangle$ and $\tilde{E}_i$ represent the perturbed atomic state and the corresponding perturbed eigenenergy, respectively.

To compute $|\Psi_i\rangle$ and $|\tilde{\Psi}_i\rangle$ we use RCC [30] and PRCC [22–27] theories, respectively. In the RCC theory the ground-state atomic wave function of a closed-shell atom is

$$|\Psi_0\rangle = e^{T^{(0)}}|\Phi_0\rangle, \tag{6}$$

where $|\Phi_0\rangle$ is the reference state wave function and $T^{(0)}$ is the cluster operator. The perturbed ground state, based on the PRCC theory, is

$$|\tilde{\Psi}_0\rangle = e^{T^{(0)}+\lambda\mathbf{T}^{(1)}\cdot\mathbf{E}}|\Phi_0\rangle = e^{T^{(0)}}[1 + \lambda\mathbf{T^{(1)}}\cdot\mathbf{E}_{\rm ext}]|\Phi_0\rangle. \tag{7}$$

For an N-electron closed-shell atom $T^{(0)} = \sum_{i=1}^{N} T_i^{(0)}$ and $\mathbf{T}^{(1)} = \sum_{i=1}^{N}\mathbf{T}_i^{(1)}$, where i is the order of excitation. An approximation, which captures most of the correlation effects, is the coupled-cluster single and double (CCSD) approximation [39]. With this approximation,

$$T^{(0)} = T_1^{(0)} + T_2^{(0)}, \tag{8a}$$

$$\mathbf{T}^{(1)} = \mathbf{T}_1^{(1)} + \mathbf{T}_2^{(1)}. \tag{8b}$$

These cluster operators in second quantized notations are

$$T_1^{(0)} = \sum_{a,p} t_a^p a_p^\dagger a_a, \tag{9a}$$

$$T_2^{(0)} = \frac{1}{4}\sum_{a,b,p,q} t_{ab}^{pq} a_p^\dagger a_q^\dagger a_b a_a, \tag{9b}$$

$$\mathbf{T}_1^{(1)} = \sum_{a,p}\tau_a^p\mathbf{C}_1(\hat{r})a_p^\dagger a_a, \tag{9c}$$

$$\mathbf{T}_2^{(1)} = \frac{1}{4}\sum_{a,b,p,q}\sum_{l,k}\tau_{ab}^{pq}(l,k)\{\mathbf{C}_l(\hat{r}_1)\mathbf{C}_k(\hat{r}_2)\}^1 a_p^\dagger a_q^\dagger a_b a_a, \tag{9d}$$

where $t_{\cdots}^{\cdots}$ and $\tau_{\cdots}^{\cdots}$ are the cluster amplitudes, $a_i^\dagger$ (a_i) are single-particle creation (annihilation) operators, and $abc\ldots$ ($pqr\ldots$) represent core (virtual) single-particle states or orbitals. Here, we have used $\mathbf{C}$ tensors to represent the perturbed cluster amplitudes to incorporate the rank of $\mathbf{D}$ in the perturbation Hamiltonian. Besides this modification, $\mathbf{T}_2^{(1)}$ are also constrained by the parity and triangular conditions [23]: $(-1)^{(l_a+l_p)} = (-1)^{(l_b+l_q)}$; $|j_a - j_p| \leqslant l \leqslant (j_a + j_p)$, $|j_b - j_q| \leqslant k \leqslant (j_b + j_q)$, and $|l-k| \leqslant 1 \leqslant (l+k)$, where $l(j)$ represents the orbital (total) angular momentum of the single-electron state.

The unperturbed cluster operators $T^{(0)}$ used in Eq. (6) are obtained by solving the coupled nonlinear equations:

$$\langle\Phi_a^p|H_{\rm N} + [H_N, T^{(0)}] + \frac{1}{2!}[[H_N, T^{(0)}], T^{(0)}] + \frac{1}{3!}[[[H_N, T^{(0)}], T^{(0)}], T^{(0)}]|\Phi_0\rangle = 0, \tag{10a}$$

$$\langle\Phi_{ab}^{pq}|H_{\rm N} + \frac{1}{2!}[[H_N, T^{(0)}], T^{(0)}] + \frac{1}{3!}[[[H_N, T^{(0)}], T^{(0)}], T^{(0)}] + \frac{1}{4!}[[[[H_N, T^{(0)}], T^{(0)}], T^{(0)}], T^{(0)}]|\Phi_0\rangle = 0. \tag{10b}$$

The states $|\Phi_a^p\rangle$ and $|\Phi_{ab}^{pq}\rangle$ are singly and doubly excited determinants obtained by replacing *one* and *two* electrons from core orbitals in $|\Phi_0\rangle$ with virtual electrons, respectively. And, $H_{\rm N} = H^{\rm DCB} - \langle\Phi_0|H^{\rm DCB}|\Phi_0\rangle$ is the normal-ordered Hamiltonian. These equations are solved first and the cluster amplitudes so obtained incorporate the electron-electron correlation effects arising from the Coulomb and Breit interactions to all orders. Similarly, the operators $\mathbf{T}^{(1)}$ in Eq. (7) are the solutions of the coupled equations,

$$\left\langle\Phi_a^p\right|H_{\rm N} + [H_N, \mathbf{T}^{(1)}] + [[H_N, T^{(0)}], \mathbf{T}^{(1)}] + \frac{1}{2!}[[[H_N, T^{(0)}], T^{(0)}], \mathbf{T}^{(1)}]|\Phi_0\rangle = \left\langle\Phi_a^p\right|[\mathbf{D}, T^{(0)}] + \frac{1}{2!}[[\mathbf{D}, T^{(0)}], T^{(0)}]|\Phi_0\rangle, \quad (11a)$$

$$\left\langle\Phi_{ab}^{pq}\right|H_{\rm N} + [H_N, \mathbf{T}^{(1)}] + [[H_N, T^{(0)}], \mathbf{T}^{(1)}] + \frac{1}{2!}[[[H_N, T^{(0)}], T^{(0)}], \mathbf{T}^{(1)}] + \frac{1}{3!}[[[[H_N, T^{(0)}], T^{(0)}], T^{(0)}], \mathbf{T}^{(1)}]|\Phi_0\rangle$$
$$= \left\langle\Phi_{ab}^{pq}\right|[\mathbf{D}, T^{(0)}] + \frac{1}{2!}[[\mathbf{D}, T^{(0)}], T^{(0)}]|\Phi_0\rangle. \quad (11b)$$

We refer to the above equations as the PRCC equations for singles and doubles, respectively. These are coupled linear equations, but nonlinear in $T^{(0)}$. More precisely, the left-hand side of the singles (doubles) equation contain terms which are two (three) orders in $T^{(0)}$. This is to account for the correlation effects associated with $H_{\rm int}$ more accurately. We solve these equations using the Jacobi method, and to remedy the slow convergence of this method we employ direct inversion of the iterated subspace (DIIS) [40].

Solving the PRCC equations is, however, computationally expensive. This is due to the large number of many-body diagrams arising from the contraction with multiple $T^{(0)}$ operators. But, in most of the cases the contribution from the nonlinear terms is very small. In such cases, only the terms linear in $T^{(0)}$ can incorporate most of the correlation effects. Then, Eq. (11) are simplified to

$$\left\langle\Phi_a^p\right|H_{\rm N} + [H_N, \mathbf{T}^{(1)}]|\Phi_0\rangle = \left\langle\Phi_a^p\right|[\mathbf{D}, T^{(0)}]|\Phi_0\rangle, \quad (12a)$$

$$\left\langle\Phi_{ab}^{pq}\right|H_{\rm N} + [H_N, \mathbf{T}^{(1)}]|\Phi_0\rangle = \left\langle\Phi_{ab}^{pq}\right|[\mathbf{D}, T^{(0)}]|\Phi_0\rangle. \quad (12b)$$

We refer to these equations as the linearized perturbed coupled-cluster (LPRCC) equations. The LPRCC incorporates all the important many-body effects like random-phase approximation and provides a good description of the atomic properties in the presence of the perturbation. In our previous works on the dipole polarizability for closed-shell systems [22–27], we have demonstrated that α obtained using LPRCC agrees well with the available theory and experimental data.

In the PRCC theory, the ground-state dipole polarizability of close-shell atoms or ions is [27]

$$\alpha = -\frac{\langle\tilde{\Psi}_0|\mathbf{D}|\tilde{\Psi}_0\rangle}{\langle\tilde{\Psi}_0|\tilde{\Psi}_0\rangle}. \quad (13)$$

From Eq. (7), using the expression of $|\tilde{\Psi}_0\rangle$ we can write

$$\alpha = -\frac{\langle\Phi_0|\mathbf{T}^{(1)\dagger}\bar{\mathbf{D}} + \bar{\mathbf{D}}\mathbf{T}^{(1)}|\Phi_0\rangle}{\langle\Psi_0|\Psi_0\rangle}, \quad (14)$$

where $\bar{\mathbf{D}}, = e^{T^{(0)\dagger}}\mathbf{D}e^{T^{(0)}}$, and in the denominator $\langle\Psi_0|\Psi_0\rangle$ is the normalization factor. Considering the computational complexity, we truncate $\bar{\mathbf{D}}$ and the normalization to factor to second order in the cluster amplitudes. Based on earlier studies, the contributions from the higher order terms are negligible [26,27]. To further improve the results we also incorporate the triply excited cluster amplitudes $\mathbf{T}_3^{(1)}$ perturbatively [27]. And, the results so obtained are labeled as PRCC(T).

III. CALCULATIONAL DETAILS

The use of basis set with good descriptions of single-electron wave functions and energies is critical to get accurate results from RCC and PRCC computations. In this work we use the Gaussian-type orbitals (GTOs) [35] as the single-electron basis for RCC and PRCC computations. The GTOs are finite basis set orbitals in which the orbitals are expressed as linear combinations of Gaussian-type functions (GTFs). Specially, the GTFs of the large component of the orbitals have the form,

$$g_{\kappa p}^L(r) = C_{\kappa i}^L r^{n_\kappa} e^{-\alpha_p r^2}, \quad (15)$$

where $p = 0, 1, 2, \ldots, m$ is the GTO index and m is the number of GTFs. And, the exponent $\alpha_p = \alpha_0\beta^{p-1}$, where α_0 and β are two independent parameters optimized separately for each orbital symmetries. This choice of the exponents is referred to as the even-tempered basis set. The small components of orbitals are derived from the large components using the kinetic balance condition [36]. To incorporate the effects of the finite size of the nucleus we use two-parameter finite size Fermi density distribution,

$$\rho_{\rm nuc}(r) = \frac{\rho_0}{1 + e^{(r-c)/a}}, \quad (16)$$

where $a = t4\ln(3)$. The parameter c is the half charge radius of the nucleus so that $\rho_{\rm nuc}(c) = \rho_0/2$, and t is the skin thickness.

To generate GTO basis we optimize α_0 and β parameters so that the orbital energies, both the core and virtual orbitals, match the numerical orbitals obtained from the CRASP2K code [41]. In addition, we also match the self-consistent field (SCF) energies. It must be mentioned here that the virtual orbitals in d (for Al^+ and Ga^+) and f (for Ga^+, In^+, and Tl^+) symmetries have significant contributions to the dipole polarizability. Hence, it is essential to optimize the virtual orbitals in d and f symmetries. The optimized α_0 and β parameters for all the ions are given in Table I.

To improve the quality of single-electron basis further, we also incorporate the effects of Breit interaction, vacuum polarization, and the self-energy corrections in the basis generation. These improved orbitals are then used in RCC and PRCC computations. This leads to, through a change in the cluster amplitudes, a small but important change in the dipole polarizability of all the ions.

TABLE I. The α_0 and β parameters of the even tempered GTO basis used in our calculations.

	s		*p*		*d*	
Ion	α_0	β	α_0	β	α_0	β
B^+	0.0046	2.258				
Al^+	0.0020	2.038	0.0020	2.105		
Ga^+	0.0046	2.258	0.0048	2.215	0.0045	2.120
In^+	0.0053	1.862	0.0052	1.870	0.0058	1.880
Tl^+	0.0570	1.895	0.0498	1.820	0.0615	1.955

IV. RESULTS AND DISCUSSIONS

The SCF and single-electron energies from optimized GTO match very well with the GRASP2K results for all the ions. The largest deviation in the SCF energy is of the order 10^{-3} hartree and this is observed in the case of In^+. For the remaining ions the deviation is much smaller, and lowest is in the case of B^+ where the deviation is of order 10^{-6} hartree. The detailed discussions on SCF and orbital energies, and the contributions from the Breit interaction, vacuum polarization, and the self-energy corrections are given in the Appendix. For comparison, we also computed the contribution from Breit interaction and vacuum polarization to the SCF energies obtained from the B-spline basis using the code by Zatsarinny and Fischer [42]. Overall the sign and magnitude of our results with GTOs are in very good agreement with the B-spline results for all the ions.

In Table II we list the values of α obtained from our computations. And, for comparison, the results from previous works are also listed in the table. As seen from the table, the LPRCC values of α are on average $\approx$24% larger than the previous theoretical results for all the ions. This is in contrast to the trends observed in our previous works [22–27], where we showed that LPRCC results are reliable for the ground-state polarizability for closed-shell systems. This could be due to the larger electron-correlation effects associated with the two-valence nature of these ions, which is further enhanced due to the orbital contraction as these are singly charged ions. To account for the strong correlation effects, in the present work, we include the nonlinear terms in PRCC theory. This accounts for the electron correlation effects arising from the perturbation more accurately through the coupling with $\mathbf{T}_1^{(1)}$ cluster operators. More precisely, from our computations we find a large cancellation due to the contribution from a nonlinear diagram arising from the PRCC term $\overline{\overline{H_N T_2^{(0)}}}\mathbf{T}_1^{(1)}$. And, hence, it reduces the value of α, which is identified as PRCC in the table.

In terms of correlation effects, as mentioned earlier, one major advantage with PRCC theory is that it does not use the sum-over-state approach [32–34]. The latter is a widely used technique to compute the dipole polarizability by summing over a selected set of intermediate states. So, the accuracy of this approach is limited by the number of excited states included in the summation. For divalent atomic systems, like the present case of group-13 ions, it is often difficult to obtain a large set of intermediate states, and this leads to errors in the computed properties. In PRCC, the summation over all the possible intermediate states within a chosen basis set is subsumed in the perturbed cluster amplitudes. Thus, it circumvents the need to compute a large set of intermediate states and this translates into improved accuracy.

TABLE II. The final value of α (in a.u.) from our calculations are compared with the other theory and experimental results. The values of α listed from present work include the effects of Breit interaction, vacuum polarization, and the self-energy corrections.

Ion	Present work	Method	Previous works	Method
B^+	12.809	LPRCC	9.62 [16]	CI+all-order
	9.413	PRCC	9.57 [43]	CCD+ST(CCD)
	9.415(56)	PRCC(T)	9.64(3) [44]	CICP
Al^+	28.624	LPRCC	24.05 [16]	CI+all-order
	23.502	PRCC	24.14(8) [45]	RCC
	23.516(141)	PRCC(T)	23.78(15)[a] [46]	Finite-field
			24.07(41)[b] [46]	Finite-field
			24.12 [47]	CI
			24.14(12) [48]	CICP
			24.20(75) [49]	Sum-rule
			24.2 [50]	MBPT
Ga^+	21.722	LPRCC	17.95 [51]	CICP
	17.762	PRCC	18.14(44) [49]	Sum-rule
	17.814(107)	PRCC(T)		
In^+	30.167	LPRCC	24.01 [16]	CI+all-order
	24.398	PRCC	24.16(3)[c] [52]	Finite-field
	24.467(147)	PRCC(T)	24.33(15)[d] [52]	Finite-field
			18.8(13) [49]	Sum-rule
Tl^+	22.834	LPRCC	19.60 [17]	CI+all-order
	20.113	PRCC	12.7(12) [49]	Sum-rule
	20.129(121)	PRCC(T)		

[a]Finite-field using energies from RCI calculations.
[b]Finite-field using energies from RCC calculations.
[c]Finite-field using energies from RCI calculations.
[d]Finite-field using energies from RCC calculations.

The next important correlation effects, in addition to the relativistic effects and Breit interactions which we include through the DCB Hamiltonian, arise from the vacuum polarization and the self-energy. The details related to the implementation of these are provided in Appendix A. In Table III we give the contributions to α from the DC Hamiltonian and each of the other terms. As we observe from the table, the contributions from the Breit interaction and vacuum polarization are opposite in phase to the DC value, and hence reduce

TABLE III. Separate contributions to α from different interaction terms in the Hamiltonian used in PRCC calculations.

Method	Al^+	Ga^+	In^+	Tl^+
PRCC(DC)	23.9989	18.0556	24.7449	20.2159
Breit int.	−0.4994	−0.3006	−0.3647	−0.1283
Vacuum pol.	−0.0004	−0.0018	−0.0070	−0.0274
Self-energy	0.0028	0.0090	0.0249	0.0526
Total	23.5019	17.7621	24.3981	20.1128

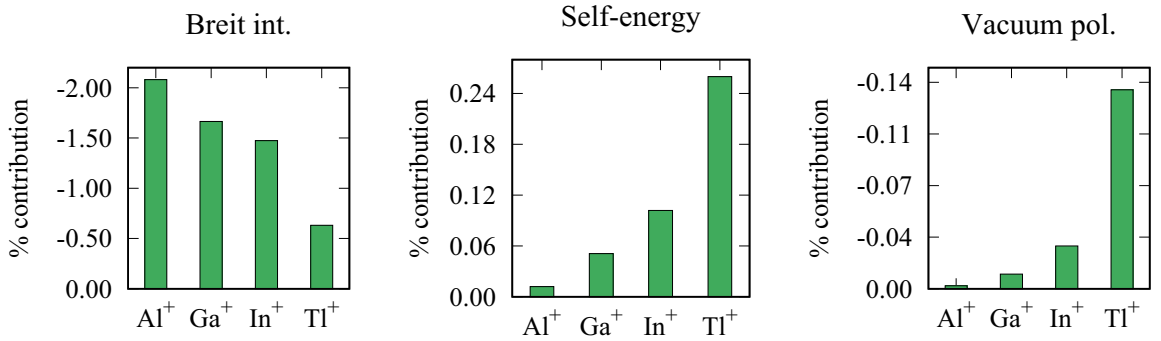

FIG. 1. The percentage contributions to α from Breit interaction, vacuum polarization, and the self-energy corrections.

the total value of α. The contribution from the self-energy correction, however, has the same phase as DC but much smaller than the Breit contribution. For quick comparison, we show the percentage contributions from these interactions in Fig. 1. As seen from the figure, the contributions are not negligible. The largest contribution from the Breit interaction is in the case of Al^+ and it is $\approx$2.1%. This is consistent with Ref. [16], where Safronova *et al.* estimated the contribution to BBR shift for Al^+ as 1.4%. This estimate is, however, using the Breit interaction at the level of the single-particle basis. In the present case, we use the DCB Hamiltonian at all steps of computations in the PRCC theory. The largest contributions from the self-energy and vacuum polarization are in the case of Tl^+, and these are $\approx$0.3% and 0.1%, respectively. To the best our knowledge, there are no previous results for group-13 ions which include corrections from vacuum polarization, self-energy, and consistent inclusion of Breit interaction. The combined contribution from these interactions are $\approx$2.1%, 1.7%, 1.6%, and 1.1%, respectively for Al^+, Ga^+, In^+, and Tl^+ ions. This suggests that these interactions must be included in the many-body calculations to obtain the accurate value of α for group-13 ions.

To further improve the accuracy of our calculations, we include the $T_3^{(0)}$ perturbatively in the PRCC computations. The details related to the inclusion of $T_3^{(0)}$ in RCC and PRCC are given in our previous works, Refs. [26,27]. The perturbative $T_3^{(0)}$ are the efficient way to incorporate the effects of triple excitations in coupled-cluster many-body calculations for two main reasons: First, it incorporates the dominant contribution through the first-order perturbation correction, and second, it is computationally less expensive than the full triples calculations. In Table II the value of α with perturbative $T_3^{(0)}$ are listed as the PRCC(T). We find that the largest contribution is in the case of Ga^+ and it is $\approx$0.3% of the PRCC value. This is small but not negligible. Hence, $T_3^{(0)}$ is included in the coupled-cluster computations to get accurate values of α.

A. Basis convergence

The results given in Table II are obtained by using an optimal orbital basis set for each of the ions. The orbital basis sets are chosen such that these are the minimal sets which give converged values of α. To show the convergence trend, in Table IV we give values of α for different basis sizes. As using the DCB Hamiltonian in the PRCC is more compute intensive, we use the Dirac-Coulomb (DC) Hamiltonian to determine the convergence. And, this is a suitable choice as the correlation effects associated with the Breit interaction is much smaller compared to the Coulomb interaction. For example, the computation of α for heavy ions like Tl^+ with a basis set of 156 orbitals takes more than a week with 134 threads. As discernible from the table, to obtain a converged basis we start with a moderate basis size and add orbitals in each symmetry systematically until the change in α is less

TABLE IV. Convergence pattern of α calculated using Dirac-Coulomb Hamiltonian (except for B^+) as function of the basis set size. The values listed are in atomic units (a_0^3).

No. of orbitals	Basis size	α
	B^+	
97	$(13s, 13p, 12d, 7f, 6g, 4h)$	9.292
119	$(15s, 15p, 14d, 9f, 8g, 6h)$	9.346
139	$(17s, 17p, 16d, 11f, 10g, 8h)$	9.358
168	$(20s, 20p, 19d, 13f, 12g, 10h)$	9.413
173	$(21s, 21p, 20d, 13f, 12g, 10h)$	9.413
	Al^+	
131	$(19s, 19p, 11d, 9f, 9g, 8h)$	23.618
148	$(22s, 22p, 12d, 10f, 10g, 9h)$	23.652
159	$(23s, 23p, 13d, 11f, 11g, 10h)$	23.789
166	$(24s, 24p, 14d, 12f, 11g, 10h)$	23.999
169	$(25s, 25p, 14d, 12f, 11g, 10h)$	23.999
	Ga^+	
116	$(16s, 16p, 14d, 7f, 7g, 6h)$	18.050
132	$(18s, 18p, 16d, 8f, 8g, 7h)$	18.050
152	$(20s, 20p, 18d, 10f, 10g, 8h)$	18.053
172	$(22s, 22p, 20d, 12f, 11g, 10h)$	18.056
177	$(23s, 23p, 21d, 12f, 11g, 10h)$	18.056
	In^+	
128	$(20s, 20p, 15d, 8f, 6g, 5h)$	24.748
139	$(21s, 21p, 16d, 9f, 7g, 6h)$	24.746
150	$(22s, 22p, 17d, 10f, 8g, 7h)$	24.744
162	$(22s, 22p, 17d, 12f, 10g, 10h)$	24.744
	Tl^+	
134	$(16s, 15p, 15d, 12f, 9g, 8h)$	20.026
147	$(17s, 16p, 16d, 13f, 10g, 10h)$	20.173
156	$(18s, 17p, 17d, 14f, 11g, 10h)$	20.129
161	$(19s, 18p, 18d, 14f, 11g, 10h)$	20.215
171	$(21s, 20p, 20d, 14f, 11g, 10h)$	20.216

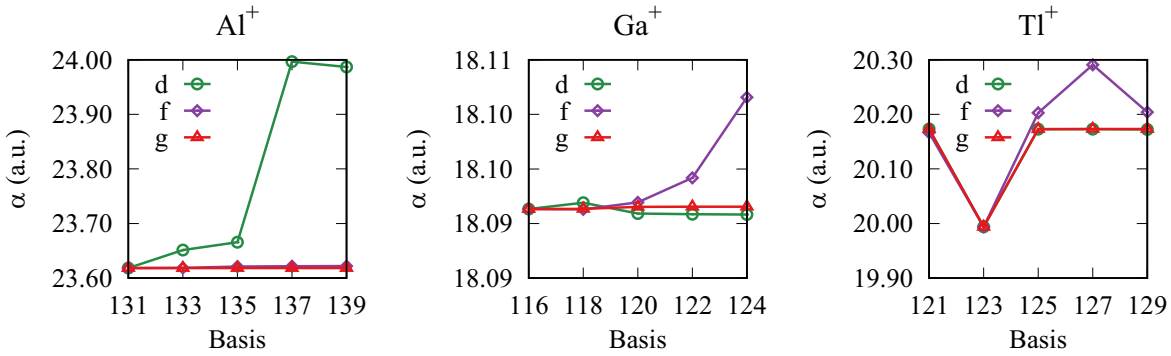

FIG. 2. The trend of contributions to α from d, f, and g virtual orbitals.

than or equal to 10^{-3} in atomic units. From the table, for example, the change in α is less than 10^{-3} for B^+ when the basis is augmented from 168 to 173. So, to minimize the computation time, we consider the basis set with 168 orbitals as optimal, and use it for the further computations to incorporate the corrections from the Breit, vacuum polarization, and self-energy interactions. Similarly, the basis with 166, 172, 150, and 161 orbitals are considered as the optimal basis for Al^+, Ga^+, In^+, and Tl^+, respectively. It is to be mentioned that the GTO basis are not, in the mathematical definition, complete. But, choosing a minimal set of exponents with well optimized α and β provides good representation for structure and properties calculations [38].

For a fine grain analysis, we compute α using basis sets with selective addition of virtual orbitals in d, f, and g symmetries. With this analysis we identify the orbital symmetry with dominant contribution to the correlation effects. To show the trend, in Fig. 2 we plot the values of α for d, f, and g symmetry with respect to the basis size. And, we see from the figure, d virtual orbitals have significant contributions for Al^+. We attribute this to the correlation effects arising from the strong mixing of $2p$ core electrons with d virtual electrons. For the other ions, Ga^+, In^+, and Tl^+, however, the dominant contribution is from the virtuals in f symmetry. This is due to the strong mixing of f virtual electrons with $3d$, $4d$, and $5d$ core electrons in the case of Ga^+, In^+, and Tl^+, respectively. This indicates that to obtain a high quality polarizability results for group-13 ions, in addition to the core orbitals, it is essential to optimize the virtual orbitals.

B. Theoretical uncertainty

In our present studies, we have identified four different sources which can contribute to the theoretical uncertainty of α. The first source is the truncation of the basis set in our computations. As mentioned earlier, the recommended values of α listed in Table II are obtained using the converged orbital basis given in Table IV. Since the change in α on augmenting the converged basis set is of the order of 10^{-3} or less, we can neglect this source of uncertainty. The second source is the truncation to the second order of $T^{(0)}$ in the expansion of $\bar{\mathbf{D}}$ in Eq. (14). In our previous work [53], using an iterative scheme, we have shown that the contribution from the remaining higher order terms is less than 0.1%. So, for this case we consider 0.1% as the upper bound. The third source is the partial inclusion of triple excitations ($\mathbf{T}_3^{(1)}$) in PRCC theory. The contributions from the perturbative triples with respect to PRCC are ≈0.06%, 0.29%, 0.28%, and 0.08% for Al^+, Ga^+, In^+, and Tl^+, respectively. Since the perturbative triples account for the dominant contribution, we select the highest contribution of 0.29% from the case of Ga^+ and take it as an upper bound to this source of uncertainty. Finally, the fourth source of theoretical uncertainty is associated with the frequency-dependent Breit interaction which we do not include in this work. However, in our previous work [26] using a series of computations with GRASP2K we estimated an upper bound of this uncertainty to be 0.13% in the case of two-valence atom Ra. Since Ra has higher Z than Tl^+, the highest-Z ion in the present work, we consider 0.13% as an upper bound to this source of uncertainty. There could be other sources of theoretical uncertainty, like the higher order coupled perturbation of vacuum polarization and self-energy terms, quadruply excited cluster operators, etc. But, these, in general, have much lower contributions and their combined theoretical uncertainty could be below 0.1%. So, combining the upper bounds of the four different sources of theoretical uncertainties, we attribute a theoretical uncertainty of 0.6% in the recommended values of α given in the present work.

C. Comparison of leading terms and interactions

To understand the general trends of the leading order contributions, we give the termwise contributions to α in Table V. From the table we observe that the leading order (LO) term is $\mathbf{T}_1^{(1)\dagger}D + \text{H.c.}$ This is to be expected as it subsumes the con-

TABLE V. Contribution to α (in a.u.) from different terms and their Hermitian conjugates from PRCC(DC) theory.

Terms + H.c.	B^+	Al^+	Ga^+	In^+	Tl^+
$\mathbf{T}_1^{(1)\dagger}\mathbf{D}$	9.9782	25.2392	19.7942	27.0396	22.3619
$\mathbf{T}_1{}^{(1)\dagger}\mathbf{D}T_2^{(0)}$	−0.3162	−0.7448	−0.6858	−1.0204	−1.1296
$\mathbf{T}_2{}^{(1)\dagger}\mathbf{D}T_2^{(0)}$	0.2740	0.6074	0.5088	0.6818	0.5700
$\mathbf{T}_1{}^{(1)\dagger}\mathbf{D}T_1^{(0)}$	−0.1804	−0.3342	−0.3222	−0.4134	−0.1352
$\mathbf{T}_2{}^{(1)\dagger}\mathbf{D}T_1^{(0)}$	0.0106	0.0206	0.0170	0.0212	−0.0078
Normalization	1.0367	1.0329	1.0696	1.0632	1.0714
Total	9.4207	23.9989	18.0556	24.7449	20.2159

tributions from the Dirac-Hartree-Fock (DHF) and the core polarization effects. The next to leading order (NLO) term is $\mathbf{T}_1{}^{(1)\dagger}DT_2^{(0)} + \text{H.c.}$ The contribution from the NLO term is opposite in phase to the LO term. And, in absolute terms it is $\approx -3\%$ each for B^+, Al^+, Ga^+, and In^+, and $\approx -5\%$ for Tl^+. The other two terms which have contributions $\approx$1% or larger are $\mathbf{T}_2{}^{(1)\dagger}DT_2^{(0)}$ and $\mathbf{T}_1{}^{(1)\dagger}DT_1^{(0)}$ terms. The contribution from the former is roughly twice than the latter but opposite in phase for all the ions. An important trend is that the contributions from terms with $\mathbf{T}_1{}^{(1)\dagger}$, namely $\mathbf{T}_1{}^{(1)\dagger}DT_2^{(0)}$ and $\mathbf{T}_1{}^{(1)\dagger}DT_1^{(0)}$, are opposite in phase to the LO term. This could be due to the correlation effects which compensates the excess contribution from the core-polarization effects subsumed in the LO term.

For comparative study of the Breit interaction, as mentioned earlier, the largest contribution is in the case of Al^+. And, from Table III one prominent trend is that the change arising from the inclusion of Breit interaction is negative and opposite to the DC. This is consistent with the previous result reported for Tl^+ [17] and our previous works [23,26,27]. As shown in Fig. 1, the contribution from the Breit interaction decreases with increasing Z of the ions. The same trend is observed in our previous works on alkaline-earth-metal atoms and the group-12 elements, where the heavier atoms Ra and Hg have smaller contributions than the lighter atoms. In absolute terms the percentage contributions to α for Al^+, Ga^+, In^+, and Tl^+ are $\approx -2.1\%$, -1.7%, -1.5%, and -0.6%, respectively.

In the case of vacuum polarization and the self-energy corrections to α, an important trend is that the contributions from these two are opposite in phase. More importantly, the same pattern is observed in our previous work on dipole polarizability of group-12 elements [27]. Quantitatively, the contribution from the self-energy is much larger and has the same phase as the LO term. In terms of actual values for Al^+ the contributions from these interactions are $\approx -0.002\%$ and 0.01% of the PRCC(DC) value, respectively. Although, there is no clear trend in the fractional contribution to α, there is a prominent pattern of increasing magnitude of the contributions from the interactions with Z. So, as to be expected, the largest contributions are in Tl^+ and these are -0.0274 and 0.0526, respectively. This indicates the importance of incorporating these effects to obtain accurate values of properties.

D. Detailed analysis

To gain better insights on the results, we compare the value of α from our calculations with previous theoretical results, and dwell on the relevant physics which can account for the differences. This is with a particular focus on the correlation effects. For clarity, we give the description for each of the ions separately. To the best of our knowledge, as mentioned earlier, there are no experimental data. It is also to be emphasized again that one major difference between previous works and the present work is that they do not include the corrections from Breit interaction, vacuum polarization, and the self-energy. Based on our results, contributions from these are not negligible. For instance, it could be as large as 2.1%, as we get in the case of Al^+, discussed earlier.

1. B^+

For B^+, there are three previous theoretical results in the literature. And, the values of α reported in these are 9.62, 9.57, and 9.64 from Safronova *et al.* [16] using CI + all-order, Archibong *et al.* [43] using CCD + ST(CCD), and Cheng *et al.* [44] using CICP, respectively. In the CI + all-order method [16], correlation effects due to valence electrons are treated using the configuration interaction (CI). And, the correlations due to the core electrons are incorporated in CI with an effective Hamiltonian obtained from the second-order perturbation theory. The upper bound on the uncertainty in the BBR shift is $\approx$10%. And, this is attributed to the Breit, core-valence correlation, and incomplete treatment of core excitations in the effective Hamiltonian, in the CI + all-order computations for B^+, Al^+, In^+, and Tl^+ ions [16,17]. The uncertainty at the level of polarizability is, however, expected to be lower than the BBR shift. In the CICP method, like the case of CI + all-order, the valence-valence correlations are treated using the CI, and the core-valence correlations are included with the help of a semiempirical core-polarization potential. The reported error in CICP value of α is about 0.3% for B^+. The other method, CCD + ST(CCD), is a much earlier work where α is computed using the perturbed energy, obtained from the coupled-cluster calculations. In the present calculation of ground-state polarizability, within the framework of PRCC, we treat group-13 ions as the closed-shell systems, and all the relevant correlations are included through cluster operators to all-orders. Our PRCC(T) result, 9.415, is about 2.1% lower than the average value of the previous three results.

2. Al^+

Among all the ions, Al^+ has the largest number of previous results. In addition to CI + all-order and CICP methods discussed above, α for Al^+ is also calculated using the RCC, CI, sum-rule, and MBPT- and RCI-based finite-field methods. Among these, in terms of mathematical formalism, the RCC method used in Kállay *et al.* [45] is closest to ours. They have used the relativistic general-order coupled-cluster theory, where the higher-order cluster excitations are considered by using the many-body diagrammatic technique-based automated programming tools. Except for the RCI-based finite-field result, 23.78 [46], the values of α reported in other works are very close to each other, and the average value is 24.10. Among the previous results, the largest and smallest theoretical errors are 3.1% and 0.3%, respectively, associated with the sum-rule [49] and RCC [45] calculations. It is, however, to be emphasized again that these results are obtained without the Breit and QED corrections. As to be expected our PRCC(DC) value of α, 23.999, without the Breit and QED corrections, matches well with the previous results. The PRCC(T) result of 23.516 is, however, 2.4% smaller than the average of the previous results. That is, the Breit and QED corrections lowers the PRCC(DC) result by 2%. And, most importantly, this is larger than the theoretical uncertainty of 0.3% reported for the RCC results. In our case, as discussed earlier, considering all the dominant contributions, the upper bound of the theoretical uncertainty is 0.6%.

3. Ga^+

For Ga^+, we found two previous results. Among these, the value of 18.14 [49] obtained using sum-rule has ≈2.4% theoretical uncertainty. The other result of 17.95 [51] using CICP seems more accurate as it has a theoretical uncertainty of ≈1.9%. These results are obtained without the Breit and QED corrections. Like in the case of Al^+, our PRCC(DC) result of 18.056 is close to the previous results. However, the PRCC(T) result of 17.814 is 0.8% and 1.8% lower than these previous results of Cheng *et al.* [51] and Reshetnikov *et al.* [49], respectively. Based on our results, the inclusion of the Breit and QED corrections lowers the PRCC(DC) results by 1.3%, which is lower than change in Al^+. This again demonstrates the importance of including Breit and QED corrections to obtain accurate values of α.

4. In^+

For In^+, there are four theoretical values of α reported in previous works. And, it is evident from the entries in Table II that there is a wide variation among the previous results. The lowest value of α is 18.8, obtained by using the sum-rule [49], while the highest value is 24.33, computed using the finite-field method based on the RCC theory [52]. The reported theoretical uncertainties in these results are 6.9% and 0.62%, respectively. The other two values, 24.16 and 24.01, using the RCI-based finite-field method from Ref. [52] and CI + all-order calculation from Safronova *et al.* [16] lie between these results. Like the previous ions, these results do not include the Breit and QED corrections. Based on our results the Breit and QED interactions lower the PRCC(DC) result by 1.4%. And, it is not surprising that our recommended value of 24.467 based on PRCC(T) is close to the RCC-based finite-field result [52], which has 0.62% theoretical uncertainty.

5. Tl^+

For Tl^+, we found two theoretical results from the published results. And, there is a large difference between these two results: The value of 19.60 obtained using CI + all-order theory [17] is 54% larger than the value of 12.7 computed using the sum-rule method [49]. The contribution from Breit interaction to α in our results is $\approx -0.6\%$. This is consistent with the estimated value of −0.5% in Ref. [17]. In the other work, Ref. [49], the error in the reported data is about 9.4%. Our PRCC(T) result, 20.129, is closer to the CI + all-order result of 19.60, however, larger by about 2.7%.

V. CONCLUSION

We have computed the ground-state electric dipole polarizability of group-13 ions using the PRCC theory. To account for the relativistic effects and QED corrections, we have used the Dirac-Coulomb-Breit Hamiltonian with the corrections from the Uehling potential and the self-energy. The effects of triple excitations are considered perturbatively. Our results from PRCC and PRCC(T) using the Dirac-Coulomb Hamiltonian are in excellent agreement with the previous results for all the ions. The results using the Dirac-Coulomb-Breit Hamiltonian are, however, lower than most of the previous results except for In^+. We attribute this to the effects of the Breit interaction, which is considered in our work but not in the previous works. The other important observation from our computations is that we need to go beyond the LPRCC to obtain accurate results for the group-13 ions. The LPRCC results are on average ≈24% larger than the PRCC results. This could be due to the strong correlation effects arising from the divalent nature of the group-13 ions. And to account for such large correlation effects the nonlinear terms in the PRCC theory must be included.

Based on our analysis of the corrections arising from the Breit interaction we find two trends. First, the contribution for all the ions are negative, and hence reduces the total value of α. The same pattern is also observed in the case of noble-gas atoms [23], alkaline-earth-metal atoms [26], and the group-12 elements [27]. In the case of singly ionized alkali-metal atoms [24], however, we get a different trend. Second, in terms of the percentage contribution, we observed the largest contribution of ≈2.1% in the case of Al^+. And, as we go towards the heavier ions the contribution decreases, the lowest is $\approx -0.63\%$, in the case of Tl^+. A similar pattern is also observed in the case of alkaline-earth-metal atoms and group-12 elements where the heavier atoms Ra and Hg have the smaller contributions, of $\approx -0.4\%$ and -0.02%, respectively, than the lighter ones. In the case of noble-gas atoms, however, we observed an opposite trend where the heaviest atom Rn has the largest contribution of ≈0.1%.

For the Uehling potential and the self-energy corrections, we observed a trend of increasing contributions from the lighter ions to the heavier ions. This is to be expected as the heavier atoms have the larger relativistic effects. The largest contributions are $\approx -0.1\%$ and 0.3% from the Uehling potential and the self-energy corrections, respectively, in the case of Tl^+. We observed an opposite trend from the Uehling potential in the case of group-12 elements [27], where Zn has larger contribution ($\approx -0.3\%$) than the Hg ($\approx -0.1\%$). For the self-energy correction, the group-12 elements show a mix behavior where both Zn and Hg have larger contribution than Cd.

To conclude, the inclusion of Breit interaction and QED corrections together contribute ≈2.1%, 1.7%, 1.6%, and 1.1%, to the ground state α of Al^+, Ga^+, In^+, and Tl^+, respectively. Based on our analysis, the upper bound on the uncertainty in our results is 0.6% for all the ions. Considering that the previous results were obtained without the inclusion of Breit and QED corrections our results have the potential to improve the estimated value of the BBR shift, and hence in the measurement of the optical clock frequency.

ACKNOWLEDGMENTS

We thank Chandan Kumar Vishwakarma for useful discussions. The results presented in the paper are based on the computations using the High Performance Computing clusters, Padum and Vikram-110 at the Indian Institute of Technology Delhi, New Delhi and Physical Research Laboratory, Ahmedabad, respectively.

APPENDIX A: BREIT INTERACTION, VACUUM POLARIZATION, AND SELF-ENERGY CORRECTIONS

For Breit interaction we use the approach introduced by Grant and Pyper [54] where the Breit interaction operator

TABLE VI. The SCF energy from GTO using the Dirac-Coulomb Hamiltonian is compared with the GRASP2K [41] results. The contributions from the Breit interaction and the vacuum polarization are compared with the results from the B-spline code [42]. All the values are in hartree.

	$E^{\rm SCF}$		$\Delta E^{\rm SCF}_{\rm Br}$		$\Delta E^{\rm SCF}_{\rm Ue}$	
Ion	GTO	GRASP2K	GTO	B-spline	GTO	B-spline
B^+	−24.24516	−24.24516	0.00148	0.00148	−0.00004	0.00005
Al^+	−242.12904	−242.12905	0.04221	0.04222	−0.00170	−0.00178
Ga^+	−1942.36249	−1942.36368	0.85161	0.85207	−0.05758	−0.05990
In^+	−5880.24254	−5880.24386	4.12196	4.12552	−0.39075	−0.40518
Tl^+	−20274.62436	−20274.62463	23.65940	23.69367	−4.11174	−4.23753

$g^B_{r_{12}}$ is expanded as a linear combination of irreducible tensor operators. We employ the expressions given in Ref. [55] to incorporate the effects of $g^B_{r_{12}}$ in single-electron basis as well as RCC and PRCC calculations. To analyze the effects of $g^B_{r_{12}}$ in detail, we compute contributions to SCF energy as well as the single-electron energies for all the ions. The correction to

TABLE VII. The orbital energies (in hartree) from GTO compared with the GRASP2K [41] results for B^+, Al^+, Ga^+, and In^+. The contributions from the Breit interaction, vacuum polarization, and the self-energy corrections to GTOs are also listed. The self-energy corrections are calculated using the code QEDMOD by Shabaev *et al.* [61]. Here [x] represents multiplication by 10^x.

Orbital	GTO	GRASP2K	$\Delta\epsilon_{\rm DC}$	$\Delta\epsilon_{\rm Br}$	$\Delta\epsilon_{\rm Ue}$	SE
			B^+			
$1s_{1/2}$	−8.18820	−8.18820	−1.078[−6]	1.205[−3]	−1.348[−5]	
$2s_{1/2}$	−0.87408	−0.87408	3.724[−8]	4.683[−5]	5.942[−7]	
			Al^+			
$1s_{1/2}$	−58.94477	−58.94478	8.394[−6]	2.723[−2]	−7.343[−4]	1.350[−2]
$2s_{1/2}$	−5.23616	−5.23616	4.048[−6]	9.664[−4]	−4.822[−5]	9.440[−4]
$2p_{1/2}$	−3.53257	−3.53258	4.032[−6]	1.723[−3]	1.136[−5]	−2.500[−5]
$2p_{3/2}$	−3.51519	−3.51520	4.458[−6]	7.349[−4]	1.136[−5]	2.000[−5]
$3s_{1/2}$	−0.65347	−0.65347	1.089[−7]	6.139[−5]	−2.642[−6]	5.900[−5]
			Ga^+			
$1s_{1/2}$	−384.21919	−384.21918	−1.465[−5]	4.854[−1]	−2.484[−2]	2.759[−1]
$2s_{1/2}$	−49.60651	−49.60652	1.478[−5]	3.530[−2]	−2.449[−3]	2.908[−2]
$2p_{1/2}$	−43.74307	−43.74302	−5.118[−5]	6.234[−2]	1.936[−4]	−7.880[−4]
$2p_{3/2}$	−42.71436	−42.71431	−4.938[−5]	4.065[−2]	2.107[−4]	1.499[−3]
$3s_{1/2}$	−6.88488	−6.88493	5.125[−5]	3.734[−3]	−3.663[−4]	4.324[−3]
$3p_{1/2}$	−4.92169	−4.92172	3.056[−5]	6.753[−3]	3.833[−5]	−6.900[−5]
$3p_{3/2}$	−4.77952	−4.77956	3.626[−5]	3.637[−3]	4.111[−5]	2.000[−4]
$3d_{3/2}$	−1.47943	−1.47940	−3.519[−5]	3.032[−4]	3.061[−5]	−1.000[−5]
$3d_{5/2}$	−1.45974	−1.45972	−2.084[−5]	8.746[−4]	3.038[−5]	1.100[−5]
$4s_{1/2}$	−0.69963	−0.69963	−3.644[−8]	2.315[−4]	−2.099[−5]	2.700[−4]
			In^+			
$1s_{1/2}$	−1033.04303	−1033.04354	5.114[−4]	2.158	−1.166[−1]	1.312
$2s_{1/2}$	−158.20733	−158.20736	3.044[−5]	1.956[−1]	−1.871[−2]	1.606[−1]
$2p_{1/2}$	−147.10243	−147.10239	−3.817[−5]	3.362[−1]	6.087[−4]	−9.080[−4]
$2p_{3/2}$	−139.31685	−139.31682	−3.620[−5]	2.276[−1]	1.086[−3]	1.316[−2]
$3s_{1/2}$	−31.67750	−31.67749	−6.513[−6]	2.699[−2]	−3.591[−3]	3.156[−2]
$3p_{1/2}$	−27.15033	−27.15031	−2.113[−5]	5.005[−2]	1.768[−4]	2.770[−4]
$3p_{3/2}$	−25.70130	−25.70128	−1.989[−5]	3.007[−2]	2.800[−4]	2.527[−3]
$3d_{3/2}$	−17.78575	−17.78573	−2.199[−5]	1.392[−2]	2.638[−4]	−2.080[−4]
$3d_{5/2}$	−17.49281	−17.49280	−3.223[−6]	5.087[−3]	2.589[−4]	2.580[−4]
$4s_{1/2}$	−5.58097	−5.58098	3.750[−6]	3.905[−3]	−6.601[−4]	5.837[−3]
$4p_{1/2}$	−4.02420	−4.02420	5.036[−7]	7.208[−3]	6.176[−5]	5.400[−5]
$4p_{3/2}$	−3.76860	−3.76860	−2.824[−6]	3.599[−3]	8.024[−5]	4.160[−4]
$4d_{3/2}$	−1.30374	−1.30375	8.368[−6]	2.132[−4]	6.288[−5]	−2.600[−5]
$4d_{5/2}$	−1.26861	−1.26861	3.999[−6]	9.058[−4]	6.182[−5]	3.200[−5]
$5s_{1/2}$	−0.63575	−0.63575	−4.827[−7]	3.259[−4]	−5.627[−5]	5.100[−4]

TABLE VIII. The orbital energies (in hartree) from GTO compared with that from the GRASP2K [41] results for Tl^+. We also provide the contributions from the Breit interaction, vacuum polarization, and the self-energy corrections. The self-energy corrections are calculated using the code QEDMOD by Shabaev *et al.* [61]. Here [x] represents multiplication by 10^x.

Orbital	GTO	GRASP2K	$\Delta\epsilon_{DC}$	$\Delta\epsilon_{Br}$	$\Delta\epsilon_{Ue}$	SE
$1s_{1/2}$	−3164.43045	−3164.43029	−1.619[−4]	11.438	−1.658	7.801
$2s_{1/2}$	−569.10850	−569.10847	−2.862[−5]	1.289	−2.369[−1]	1.190
$2p_{1/2}$	−545.21645	−545.21644	−1.574[−5]	2.168	−1.613[−2]	1.012[−1]
$2p_{3/2}$	−469.18398	−469.18397	−1.088[−5]	1.362	7.960[−3]	1.468[−1]
$3s_{1/2}$	−138.62965	−138.62966	7.600[−6]	2.397[−1]	−5.398[−2]	2.766[−1]
$3p_{1/2}$	−127.91899	−127.91900	1.550[−6]	4.140[−1]	−3.956[−3]	3.027[−2]
$3p_{3/2}$	−110.79473	−110.79474	1.850[−6]	2.461[−1]	2.336[−3]	3.545[−2]
$3d_{3/2}$	−93.35056	−93.35059	2.126[−5]	1.802[−1]	2.602[−3]	−2.150[−3]
$3d_{5/2}$	−89.72674	−89.72677	2.463[−5]	1.163[−1]	2.462[−3]	4.477[−3]
$4s_{1/2}$	−32.55930	−32.55932	1.562[−5]	4.945[−2]	−1.363[−2]	7.001[−2]
$4p_{1/2}$	−27.91070	−27.91071	1.151[−5]	8.834[−2]	−8.320[−4]	7.596[−3]
$4p_{3/2}$	−23.69397	−23.69398	1.113[−5]	4.601[−2]	7.719[−4]	8.733[−3]
$4d_{3/2}$	−16.11031	−16.11033	2.634[−5]	2.455[−2]	7.758[−4]	−5.640[−4]
$4d_{5/2}$	−15.31327	−15.31328	2.968[−6]	1.038[−2]	7.413[−4]	1.169[−3]
$4f_{5/2}$	−5.45750	−5.45748	−1.622[−5]	−5.867[−3]	5.503[−4]	0.000
$4f_{7/2}$	−5.28151	−5.28149	−2.175[−5]	−1.193[−2]	5.396[−4]	0.000
$5s_{1/2}$	−5.88606	−5.88606	−4.033[−6]	7.680[−3]	−2.652[−3]	1.377[−2]
$5p_{1/2}$	−4.25160	−4.25159	−4.585[−6]	1.333[−2]	−1.795[−5]	1.330[−3]
$5p_{3/2}$	−3.48442	−3.48442	−1.251[−6]	5.378[−3]	2.810[−4]	1.459[−3]
$5d_{3/2}$	−1.16120	−1.16120	4.185[−6]	4.544[−4]	2.194[−4]	−6.200[−5]
$5d_{5/2}$	−1.07329	−1.07330	2.670[−6]	−1.067[−3]	2.070[−4]	1.230[−4]
$6s_{1/2}$	−0.68952	−0.68952	−1.365[−6]	6.872[−4]	−3.000[−4]	1.519[−3]

single-electron energy due to Breit interaction is

$$\Delta\epsilon_{Br(i)} = \epsilon_i' - \epsilon_i, \tag{A1}$$

where ϵ_i and ϵ_i' represent the orbital energies obtained by solving the Dirac-Hartree-Fock and Dirac-Hartree-Fock-Breit orbital equations self-consistently, respectively. Similarly, the correction to the SCF energy is

$$\Delta E_{Br}^{SCF} = E_{DCB}^{SCF} - E_{DC}^{SCF}, \tag{A2}$$

where E_{DCB}^{SCF} and E_{DC}^{SCF} are the SCF energies computed using DCB and DC Hamiltonian, respectively. The ΔE_{Br}^{SCF} computed from our implementation on GTO is given in Table VI where we compare our results with a recently reported code for B-spline basis by Zatsarinny *el al.* [42]. The contributions to the orbital energies are tabulated in Tables VII (for B^+, Al^+, Ga^+, and In^+) and VIII (for Tl^+) for a quantitative description.

The effects of vacuum polarization is considered using the Uehling potential [56], which provides the leading order contribution. It must, however, be modified to include the effects of finite nuclear size [57,58] and in our present work we use the expression given in Ref. [59]. In our previous work, Ref. [25], we had discussed the details of the implementation. To quantify the effects in the present work, we compute the corrections to orbital energies as well as the SCF energy for all the ions. The correction to orbital energy is

$$\Delta\epsilon_{Ue(i)} = \epsilon_i' - \epsilon_i, \tag{A3}$$

where ϵ_i' and ϵ_i are the energies with and without Uehling potential, respectively. Similarly, the correction to SCF energy is

$$\Delta E_{Ue}^{SCF} = E_{(DC+Ue)}^{SCF} - E_{DC}^{SCF}, \tag{A4}$$

where E_{DC+Ue}^{SCF} and E_{DC}^{SCF} are the SCF energies computed using DC plus Uehling potential and DC Hamiltonian, respectively. The ΔE_{Ue}^{SCF} from our computations are tabulated and compared with the results from the B-spline code [42] in Table VI. And $\Delta\epsilon_{Ue(i)}$ are given in Tables VII and VIII.

The effects of the self-energy (SE) correction to orbitals are considered through the model Lamb-shift operator introduced by Shabaev *et al.* [60]. For this we use the code QEDMOD [61], developed by the same authors, to compute the corrections to the orbital energies. These corrections to energies are applied and used in the RCC and PRCC computations. A similar analysis was reported for the group-12 elements in our previous work [27]. The data on SE corrections to orbital energies, computed using the QEDMOD code, are listed in Tables VII and VIII.

APPENDIX B: SCF AND ORBITAL ENERGIES

In Table VI we compare the SCF energy from GTO with GRASP2K [41]. Considering the Breit correction, the sign of ΔE_{Br}^{SCF} is positive for all the ions and matches with the B-spline results. The positive sign of ΔE_{Br}^{SCF} indicates an increase in the SCF energy, which we attribute to the spatial contraction of the orbitals. Interestingly, we observed the same trend of ΔE_{Br}^{SCF} in the case of the noble-gas [23] and group-12 elements [27]. Examining the values listed in the table, we find that our GTO results are in excellent agreement with the B-spline results. The largest difference is of the order of 10^{-2} hartree, which occurs in the case Tl^+. The last

TABLE IX. The orbital energies for virtual orbitals (in hartree) from GTO is compared with the GRASP2K [41] results for Al^+ and Ga^+. Here [x] represents multiplication by 10^x.

Orbital	GTO	GRASP2K	$\Delta\epsilon$
		Al^+	
$3d_{3/2}$	−0.05791	−0.05791	4.859[−9]
$3d_{5/2}$	−0.05791	−0.05791	4.851[−9]
$4d_{3/2}$	−0.03254	−0.03254	5.076[−7]
$4d_{5/2}$	−0.03254	−0.03254	5.076[−7]
$5d_{3/2}$	−0.02072	−0.02072	4.973[−6]
$5d_{5/2}$	−0.02072	−0.02072	4.973[−6]
$6d_{3/2}$	−0.01430	−0.01433	2.706[−5]
$6d_{5/2}$	−0.01430	−0.01433	2.706[−5]
$7d_{3/2}$	−0.01039	−0.01049	9.621[−5]
$7d_{5/2}$	−0.01039	−0.01049	9.620[−5]
$8d_{3/2}$	−0.00781	−0.00800	1.975[−4]
$8d_{5/2}$	−0.00781	−0.00800	1.975[−4]
		Ga^+	
$4f_{5/2}$	−0.03126	−0.03087	−3.936[−4]
$4f_{7/2}$	−0.03126	−0.03087	−3.947[−4]
$5f_{5/2}$	−0.02001	−0.01946	−5.518[−4]
$5f_{7/2}$	−0.02001	−0.02024	2.304[−4]
$6f_{5/2}$	−0.01388	−0.01484	9.610[−4]
$6f_{7/2}$	−0.01388	−0.01406	1.798[−4]
$7f_{5/2}$	−0.01015	−0.00998	−1.695[−4]
$7f_{7/2}$	−0.01015	−0.00998	−1.672[−4]
$8f_{5/2}$	−0.00762	−0.00793	3.140[−4]
$8f_{7/2}$	−0.00762	−0.00793	−3.164[−4]
$9f_{5/2}$	−0.00584	−0.00624	−3.982[−4]
$9f_{7/2}$	−0.00584	−0.00622	−3.856[−4]
$10f_{5/2}$	−0.00484	−0.00506	2.148[−4]
$10f_{7/2}$	−0.00484	−0.00507	2.227[−4]
$11f_{5/2}$	−0.00377	−0.00410	3.231[−4]
$11f_{7/2}$	−0.00377	−0.00411	3.366[−4]
$12f_{5/2}$	−0.01273	−0.00351	−9.222[−3]
$12f_{7/2}$	−0.01273	−0.00350	−9.236[−3]

TABLE X. The orbital energies for virtual f orbitals (in hartree) from GTO are compared with the GRASP2K [41] results for In^+ and Tl^+. Here [x] represents multiplication by 10^x.

Orbital	GTO	GRASP2K	$\Delta\epsilon$
		In^+	
$4f_{5/2}$	−0.03127	−0.03127	−5.307[−8]
$4f_{7/2}$	−0.03127	−0.03127	−6.643[−8]
$5f_{5/2}$	−0.02002	−0.01985	−1.720[−4]
$5f_{7/2}$	−0.02002	−0.01978	−2.334[−4]
$6f_{5/2}$	−0.01390	−0.01407	1.736[−4]
$6f_{7/2}$	−0.01390	−0.01414	2.348[−4]
$7f_{5/2}$	−0.01021	−0.01379	3.585[−3]
$7f_{7/2}$	−0.01021	−0.01008	−1.211[−4]
$8f_{5/2}$	−0.07786	−0.07929	1.436[−4]
$8f_{7/2}$	−0.00779	−0.00795	1.621[−4]
$9f_{5/2}$	−0.00609	−0.00524	−8.482[−4]
$9f_{7/2}$	−0.00609	−0.00543	−6.567[−4]
$10f_{5/2}$	−0.00490	−0.00594	1.045[−3]
$10f_{7/2}$	−0.00490	−0.00575	8.538[−4]
		Tl^+	
$5f_{5/2}$	−0.03127	−0.02002	−1.125[−2]
$5f_{7/2}$	−0.03127	−0.02002	−1.125[−2]
$6f_{5/2}$	−0.02002	−0.01390	−6.116[−3]
$6f_{7/2}$	−0.02002	−0.01390	−6.115[−3]
$7f_{5/2}$	−0.01390	−0.01021	−3.686[−3]
$7f_{7/2}$	−0.01390	−0.01021	−3.686[−3]
$8f_{5/2}$	−0.01020	−0.00782	−2.382[−3]
$8f_{7/2}$	−0.01020	−0.00782	−2.382[−3]
$9f_{5/2}$	−0.00776	−0.00618	−1.579[−3]
$9f_{7/2}$	−0.00776	−0.00617	−1.579[−3]
$10f_{5/2}$	−0.00595	−0.00500	−9.461[−4]
$10f_{7/2}$	−0.00595	−0.00500	−9.461[−4]
$11f_{5/2}$	−0.00449	−0.00413	−3.565[−4]
$11f_{7/2}$	−0.00449	−0.00413	−3.565[−4]
$12f_{5/2}$	−0.00336	−0.00347	1.168[−4]
$12f_{7/2}$	−0.00336	−0.00347	1.165[−4]
$13f_{5/2}$	−0.00297	−0.00296	−1.145[−5]
$13f_{7/2}$	−0.00297	−0.00296	−1.203[−5]
$14f_{5/2}$	−0.01735	−0.00255	1.991[−2]
$14f_{7/2}$	−0.01735	−0.00255	1.990[−2]

two columns of Table VI show the comparison of $\Delta E_{\rm Ue}^{\rm SCF}$ from GTO with the B-spline data. Unlike $\Delta E_{\rm Br}^{\rm SCF}$, $\Delta E_{\rm Ue}^{\rm SCF}$ from GTO has negative value for all the ions, indicating a decrease in the SCF energy. This decrease in SCF energy implies the relaxation of the orbitals. There is a sign mismatch in the results of B^+, though, the contribution is very small. For the remaining ions, both sign as well as magnitude of GTO results are in good agreement with the B-spline data.

In Tables VII and VIII we list the orbital energies of GTO and compare that with the numerical orbitals obtained from the GRASP2K. The orbital energies of core as well as virtual orbitals from GTO are in excellent agreement with the GRASP2K results for all the ions. Among the core orbitals, the largest difference between the two results is of the order of 10^{-4} hartree, in the case of $1s_{1/2}$ orbitals of In^+ and Tl^+. For all other orbitals, in all the ions, the difference is even smaller. Among the virtuals, as shown in Tables IX and X, the largest difference of the order of 10^{-2} hartree is observed in the case of $5f$ of Tl^+.

Examining the contributions to orbital energies from the Breit interaction, $\Delta\epsilon_{\rm Br}$ is positive for all the orbitals in all the ions. This indicates the relaxation of the orbitals. A similar trend was also found in our previous work on group-12 elements [27]. When we compare the values of $\Delta\epsilon_{\rm Br}$, we observe two important trends. First, as to be expected, the inner core orbitals have the larger corrections. For instance, $\Delta\epsilon_{\rm Br}$, 4.854×10^{-1} hartree, for $1s_{1/2}$ orbital in Ga^+ is three orders of magnitude larger than that of 2.315×10^{-4} for $4s_{1/2}$. As we observe from the tables, this difference is larger in the case of heavier ions In^+ and Tl^+. Second, $\Delta\epsilon_{\rm Br}$ increases with Z. For instance, $\Delta\epsilon_{\rm Br}$ in Tl^+ is ≈5, 7, 9, 12, and 23 times larger in magnitude than In^+ for $1s_{1/2}$, $2s_{1/2}$, $3s_{1/2}$, $4s_{1/2}$, and $5s_{1/2}$ orbitals, respectively.

Looking into the contributions from the Uehling potential, we find that the s orbitals in all the ions and $p_{1/2}$ orbitals in Tl^+ tend to contract. This is an important difference from the Breit contribution. The other important point to observe is that $\Delta\epsilon_{\rm Ue}$ is smaller than $\Delta\epsilon_{\rm Br}$ for all the states in all the ions. In

terms of actual contribution within an ion, similar to the trend of Breit interaction, $\Delta\epsilon_{\rm Ue}$ for inner cores are larger than the outer core orbitals. This trend is to be expected as the vacuum polarization being an attractive and short-range potential has the large effects on the orbitals with finite probability density within the nucleus.

Considering the contributions from the self-energy to the orbital energies, they are negligibly small in the case of B^+. So, we do not provide the contributions for B^+. As we observe from the tables for other ions, like Breit interaction and vacuum polarization corrections, the self-energy correction SE also is largest for the inner cores, and decreases for orbitals with higher principal quantum numbers. This is because the inner core orbitals have the larger relativistic effects. Looking in terms of the signs of SE, we observe a mix trend. The SE in negative for $p_{1/2}$ and $d_{3/2}$ orbitals in the case of Al^+, Ga^+, and In^+ ions. However, it is negative only for $p_{1/2}$ orbitals in the case of In^+. In terms of the magnitude of the corrections from Al^+ to Tl^+, as to be expected, it increases with Z.

[1] K. D. Bonin and V. V. Kresin, *Electric-Dipole Polarizabilities of Atoms, Molecules and Clusters* (World Scientific, Singapore, 1997).

[2] I. B. Khriplovich, *Parity Nonconservation in Atomic Phenomena* (Gordon and Breach Science Publishers, Philadelphia, 1991).

[3] W. C. Griffith, M. D. Swallows, T. H. Loftus, M. V. Romalis, B. R. Heckel, and E. N. Fortson, Improved Limit on the Permanent Electric Dipole Moment of Hg^{199}, Phys. Rev. Lett. **102**, 101601 (2009).

[4] Th. Udem, R. Holzwarth, and T. W. Hansch, Optical frequency metrology, Nature (London) **416**, 233 (2002).

[5] S. A. Diddams, J. C. Bergquist, S. R. Jefferts, and C. W. Oates, Standards of time and frequency at the outset of the 21st century, Science **306**, 1318 (2004).

[6] M. H. Anderson, J. R. Ensher, M. R. Matthews, C. E. Wieman, and E. A. Cornell, Observation of Bose-Einstein condensation in a dilute atomic vapor, Science **269**, 198 (1995).

[7] C. C. Bradley, C. A. Sackett, J. J. Tollett, and R. G. Hulet, Evidence of Bose-Einstein Condensation in an Atomic Gas with Attractive Interactions, Phys. Rev. Lett. **75**, 1687 (1995).

[8] K. B. Davis, M. O. Mewes, M. R. Andrews, N. J. van Druten, D. S. Durfee, D. M. Kurn, and W. Ketterle, Bose-Einstein Condensation in a Gas of Sodium Atoms, Phys. Rev. Lett. **75**, 3969 (1995).

[9] M. Lewenstein, Ph. Balcou, M. Yu. Ivanov, A. L'Huillier, and P. B. Corkum, Theory of high-harmonic generation by low-frequency laser fields, Phys. Rev. A **49**, 2117 (1994).

[10] M. Lewenstein, P. Salières, and A. L'Huillier, Phase of the atomic polarization in high-order harmonic generation, Phys. Rev. A **52**, 4747 (1995).

[11] C. I. Blaga, F. Catoire, P. Colosimo, G. G. Paulus, H. G. Muller, P. Agostini, and L. F. DiMauro, Strong-field photoionization revisited, Nat. Phys. **5**, 335 (2009).

[12] Yu Hang Lai, C. I. Blaga, J. Xu, H. Fuest, P. Rupp, M. F. Kling, P. Agostini, and L. F. DiMauro, Polarizability effect in strong-field ionization: Quenching of the low-energy structure in C_{60}, Phys. Rev. A **98**, 063427 (2018).

[13] S. G. Karshenboim and E. Peik, *Astrophysics, Clocks and Fundamental Constants*, Lecture Notes in Physics (Springer, New York, 2010).

[14] H. G. Dehmelt, Mono-ion oscillator as potential ultimate laser frequency standard, IEEE Trans. Instrum. Meas. **IM-31**, 83 (1982).

[15] C. W. Chou, D. B. Hume, J. C. J. Koelemeij, D. J. Wineland, and T. Rosenband, Frequency Comparison of Two High-Accuracy Al^+ Optical Clocks, Phys. Rev. Lett. **104**, 070802 (2010).

[16] M. S. Safronova, M. G. Kozlov, and C. W. Clark, Precision Calculation of Blackbody Radiation Shifts for Optical Frequency Metrology, Phys. Rev. Lett. **107**, 143006 (2011).

[17] Z. Zuhrianda, M. S. Safronova, and M. G. Kozlov, Anomalously small blackbody radiation shift in the Tl^+ frequency standard, Phys. Rev. A **85**, 022513 (2012).

[18] J.-S. Chen, S. M. Brewer, C. W. Chou, D. J. Wineland, D. R. Leibrandt, and D. B. Hume, Sympathetic Ground State Cooling and Time-Dilation Shifts in an $^{27}Al^+$ Optical Clock, Phys. Rev. Lett. **118**, 053002 (2017).

[19] E. Fluck, New notations in the periodic table, Pure Appl. Chem. **60**, 431 (1988).

[20] S. M. Brewer, J.-S. Chen, A. M. Hankin, E. R. Clements, C. W. Chou, D. J. Wineland, D. B. Hume, and D. R. Leibrandt, $^{27}Al^+$ Quantum-Logic Clock with a Systematic Uncertainty Below 10^{-18}, Phys. Rev. Lett. **123**, 033201 (2019).

[21] S. M. Brewer, J.-S. Chen, K. Beloy, A. M. Hankin, E. R. Clements, C. W. Chou, W. F. McGrew, X. Zhang, R. J. Fasano, D. Nicolodi, H. Leopardi, T. M. Fortier, S. A. Diddams, A. D. Ludlow, D. J. Wineland, D. R. Leibrandt, and D. B. Hume, Measurements of $^{27}Al^+$ and $^{25}Mg^+$ magnetic constants for improved ion-clock accuracy, Phys. Rev. A **100**, 013409 (2019).

[22] S. Chattopadhyay, B. K. Mani, and D. Angom, Electric dipole polarizability from perturbed relativistic coupled-cluster theory: Application to neon, Phys. Rev. A **86**, 022522 (2012).

[23] S. Chattopadhyay, B. K. Mani, and D. Angom, Perturbed coupled-cluster theory to calculate dipole polarizabilities of closed-shell systems: Application to Ar, Kr, Xe, and Rn, Phys. Rev. A **86**, 062508 (2012).

[24] S. Chattopadhyay, B. K. Mani, and D. Angom, Electric dipole polarizabilities of alkali-metal ions from perturbed relativistic coupled-cluster theory, Phys. Rev. A **87**, 042520 (2013).

[25] S. Chattopadhyay, B. K. Mani, and D. Angom, Electric dipole polarizabilities of doubly ionized alkaline-earth-metal ions from perturbed relativistic coupled-cluster theory, Phys. Rev. A **87**, 062504 (2013).

[26] S. Chattopadhyay, B. K. Mani, and D. Angom, Electric dipole polarizability of alkaline-earth-metal atoms from perturbed relativistic coupled-cluster theory with triples, Phys. Rev. A **89**, 022506 (2014).

[27] S. Chattopadhyay, B. K. Mani, and D. Angom, Triple excitations in perturbed relativistic coupled-cluster theory and electric dipole polarizability of group-IIb elements, Phys. Rev. A **91**, 052504 (2015).

[28] S. G. Porsev and A. Derevianko, Multipolar theory of blackbody radiation shift of atomic energy levels and its implications for optical lattice clocks, Phys. Rev. A **74**, 020502(R) (2006).

[29] R. Pal, M. S. Safronova, W. R. Johnson, A. Derevianko, and S. G. Porsev, Relativistic coupled-cluster single-double method applied to alkali-metal atoms, Phys. Rev. A **75**, 042515 (2007).

[30] B. K. Mani, K. V. P. Latha, and D. Angom, Relativistic coupled-cluster calculations of ^{20}Ne, ^{40}Ar, ^{84}Kr, and ^{129}Xe: Correlation energies and dipole polarizabilities, Phys. Rev. A **80**, 062505 (2009).

[31] H. S. Nataraj, B. K. Sahoo, B. P. Das, and D. Mukherjee, Reappraisal of the Electric Dipole Moment Enhancement Factor for Thallium, Phys. Rev. Lett. **106**, 200403 (2011).

[32] M. S. Safronova, W. R. Johnson, and A. Derevianko, Relativistic many-body calculations of energy levels, hyperfine constants, electric-dipole matrix elements, and static polarizabilities for alkali-metal atoms, Phys. Rev. A **60**, 4476 (1999).

[33] A. Derevianko, W. R. Johnson, M. S. Safronova, and J. F. Babb, High-Precision Calculations of Dispersion Coefficients, Static Dipole Polarizabilities, and Atom-Wall Interaction Constants for Alkali-Metal Atoms, Phys. Rev. Lett. **82**, 3589 (1999).

[34] J. Mitroy, M. S. Safronova, and C. W. Clark, Theory and applications of atomic and ionic polarizabilities, J. Phys. B **43**, 202001 (2010).

[35] A. K. Mohanty, F. A. Parpia, and E. Clementi, Kinetically balanced geometric Gaussian basis set calculations for relativistic many-electron atoms, in *Modern Techniques in Computational Chemistry: MOTECC-91*, edited by E. Clementi (ESCOM, Leiden, 1991).

[36] R. E. Stanton and S. Havriliak, Kinetic balance: A partial solution to the problem of variational safety in Dirac calculations, J. Chem. Phys. **81**, 1910 (1984).

[37] I. P. Grant, *Relativistic Quantum Theory of Atoms and Molecules: Theory and Computation* (Springer, New York, 2010).

[38] I. Grant, Relativistic atomic structure, in *Springer Handbook of Atomic, Molecular, and Optical Physics*, edited by G. Drake (Springer, New York, 2006), pp. 325–357.

[39] G. D. Purvis and R. J. Bartlett, A full coupled cluster singles and doubles model: The inclusion of disconnected triples, J. Chem. Phys. **76**, 1910 (1982).

[40] P. Pulay, Convergence acceleration of iterative sequences. the case of scf iteration, Chem. Phys. Lett. **73**, 393 (1980).

[41] P. Jönsson, G. Gaigalas, J. Bieroń, C. Froese Fischer, and I. P. Grant, New version: Grasp2k relativistic atomic structure package, Comp. Phys. Comm. **184**, 2197 (2013).

[42] O. Zatsarinny and C. F. Fischer, DBSR$_{\rm HF}$: A B-spline Dirac-Hartree-Fock program, Comput. Phys. Commun. **202**, 287 (2016).

[43] E. F. Archibong and A. J. Thakkar, Hyperpolarizabilities and polarizabilities of Li^{-1} and B^{+}: Finite-field coupled-cluster calculations, Chem. Phys. Lett. **173**, 579 (1990).

[44] Y. Cheng and J. Mitroy, Blackbody radiation shift of the B^{+} clock transition, Phys. Rev. A **86**, 052505 (2012).

[45] M. Kállay, H. S. Nataraj, B. K. Sahoo, B. P. Das, and L. Visscher, Relativistic general-order coupled-cluster method for high-precision calculations: Application to the Al^{+} atomic clock, Phys. Rev. A **83**, 030503(R) (2011).

[46] Y. M. Yu, B. B. Suo, and H. Fan, Finite-field calculation of the polarizabilities and hyperpolarizabilities of Al^{+}, Phys. Rev. A **88**, 052518 (2013).

[47] L. Hamonou and A. Hibbert, Static and dynamic polarizabilities of Mg-like ions, J. Phys. B **41**, 245004 (2008).

[48] J. Mitroy, J. Y. Zhang, M. W. J. Bromley, and K. G. Rollin, Blackbody radiation shift of the Al^{+} clock transition, Eur. Phys. J. D **53**, 15 (2009).

[49] N. Reshetnikov, L. J. Curtis, M. S. Brown, and R. E. Irving, Determination of polarizabilities and lifetimes for the Mg, Zn, Cd and Hg isoelectronic sequences, Phys. Scr. **77**, 015301 (2008).

[50] E. F. Archibong and A. J. Thakkar, Finite-field many-body-perturbation-theory calculation of the static hyperpolarizabilities and polarizabilities of Mg, Al^{+}, and Ca, Phys. Rev. A **44**, 5478 (1991).

[51] Y. Cheng and J. Mitroy, Blackbody radiation shift of the Ga^{+} clock transition, J. Phys. B: At., Mol. Opt. Phys. **46**, 185004 (2013).

[52] Y. M. Yu, B. B. Suo, H. H. Feng, H. Fan, and W. M. Liu, Finite-field calculation of static polarizabilities and hyperpolarizabilities of In^{+} and Sr, Phys. Rev. A **92**, 052515 (2015).

[53] B. K. Mani and D. Angom, Atomic properties calculated by relativistic coupled-cluster theory without truncation: Hyperfine constants of Mg^{+}, Ca^{+}, Sr^{+}, and Ba^{+}, Phys. Rev. A **81**, 042514 (2010).

[54] I. P. Grant and N. C. Pyper, Breit interaction in multiconfiguration relativistic atomic calculations, J. Phys. B **9**, 761 (1976).

[55] I. P. Grant and B. J. McKenzie, The transverse electron-electron interaction in atomic structure calculations, J. Phys. B **13**, 2671 (1980).

[56] E. A. Uehling, Polarization effects in the positron theory, Phys. Rev. **48**, 55 (1935).

[57] L. W. Fullerton and G. A. Rinker, Accurate and efficient methods for the evaluation of vacuum-polarization potentials of order $z\alpha$ and $z\alpha^2$, Phys. Rev. A **13**, 1283 (1976).

[58] S. Klarsfeld, Analytical expressions for the evaluation of vacuum-polarization potentials in muonic atoms, Phys. Lett. B **66**, 86 (1977).

[59] W. R. Johnson, I. Bednyakov, and G. Soff, Vacuum-Polarization Corrections to the Parity-Nonconserving $6s-7s$ Transition Amplitude in ^{133}Cs, Phys. Rev. Lett. **87**, 233001 (2001).

[60] V. M. Shabaev, I. I. Tupitsyn, and V. A. Yerokhin, Model operator approach to the lamb shift calculations in relativistic many-electron atoms, Phys. Rev. A **88**, 012513 (2013).

[61] V. M. Shabaev, I. I. Tupitsyn, and V. A. Yerokhin, QEDMOD: Fortran program for calculating the model lamb-shift operator, Comput. Phys. Commun. **189**, 175 (2015).